

Topological and Multipolar Magnets and Spintronics

Satoru Nakatsuji

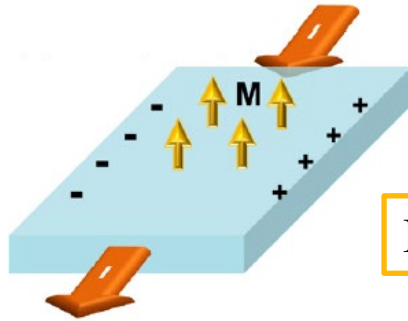
Dept. of Physics, University of Tokyo
Institute for Solid State Physics (ISSP), University of Tokyo
Institute of Quantum Matters (IQM), Johns Hopkins University

Plan

- Multipole Physics on Correlated Electron Systems
- Topological States in Magnetic Systems
- Physics of Antiferromagnetic Weyl Semimetals
- Physics of Multipolar Kondo Lattice Systems

Order parameters characterizing AHE

● Ferromagnets

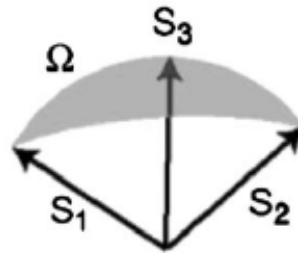
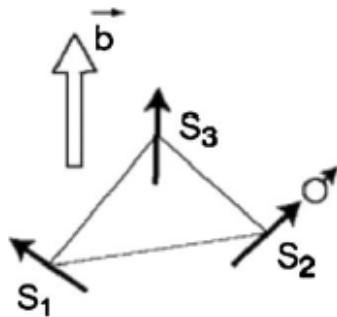


Ferromagnets exhibit AHE in the presence of S-O coupling.

Karplus and Luttinger, Phys. Rev. **95**, 1154 (1954)

Figure from C.-Z. Chang and M. Li. (2016)

● Non-coplanar ferromagnets

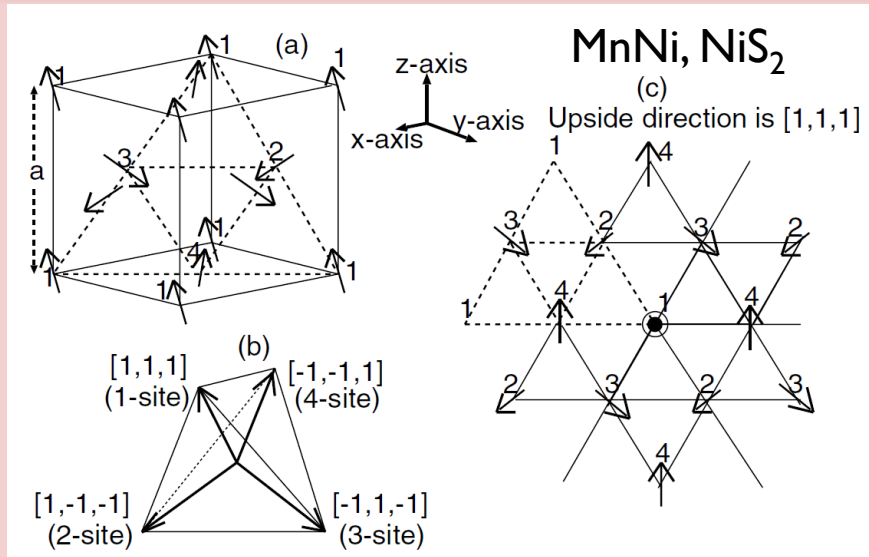


$$\chi_{ijk} = \vec{S}_i \cdot (\vec{S}_j \times \vec{S}_k)$$

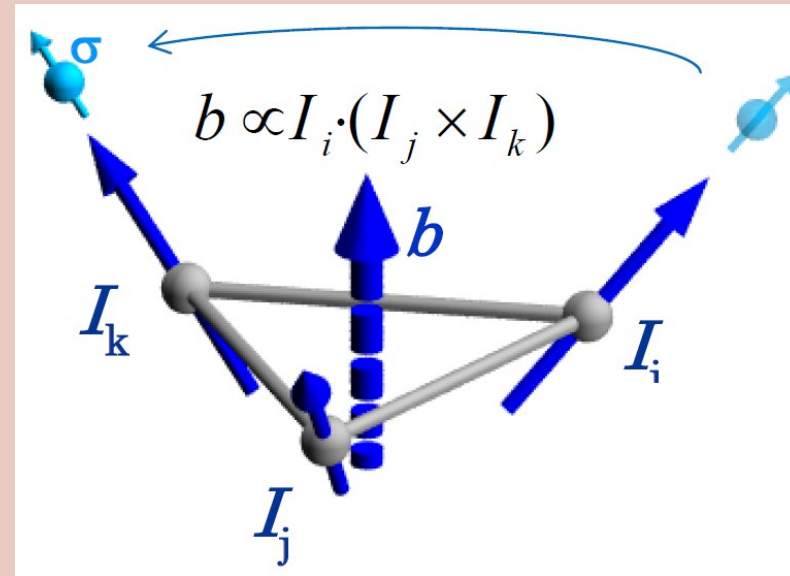
Finite scalar spin chirality induces the AHE.

Shindou and Nagaosa, Phys. Rev. Lett. **87**, 116801 (2001).

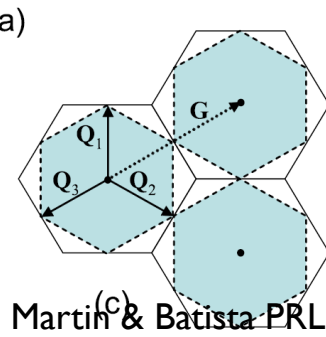
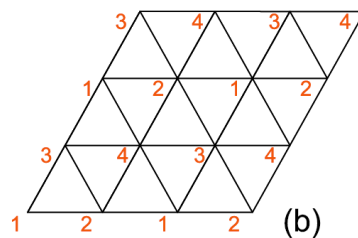
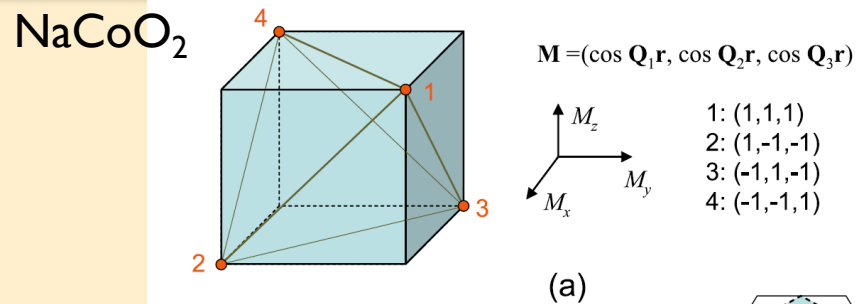
Theory: AHE in AFM



Shindou & Nagaosa PRL (2001).

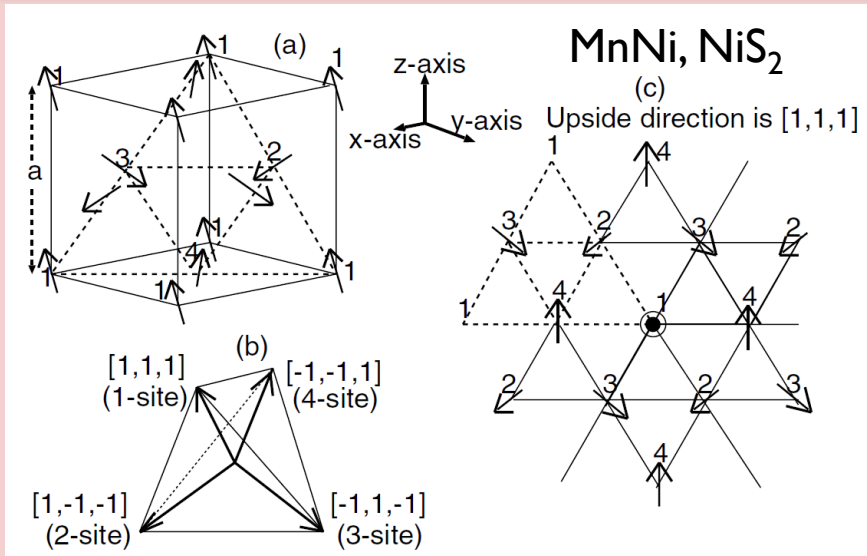


Spin Chirality Mechanism

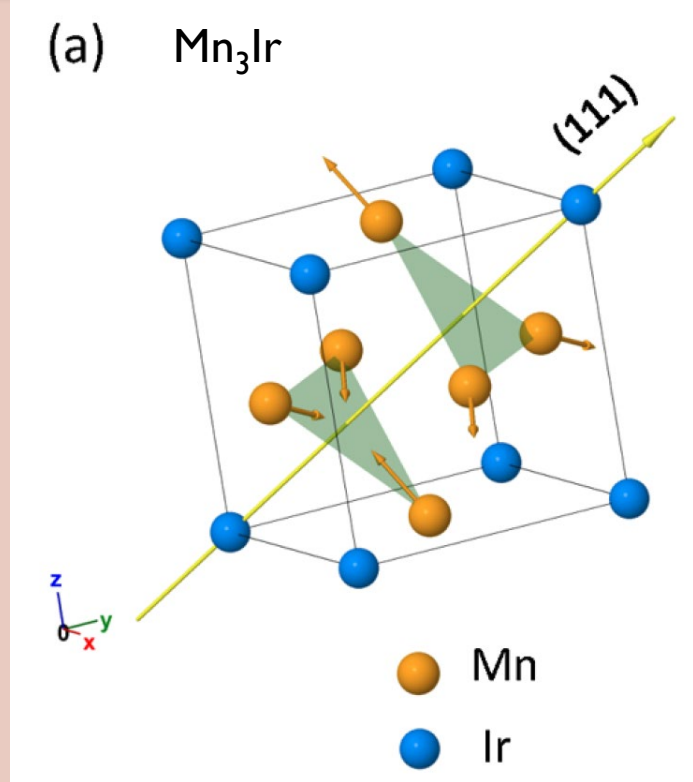


Martin & Batista PRL (2008).

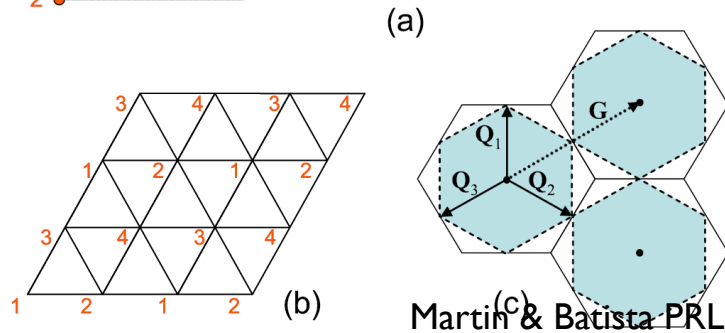
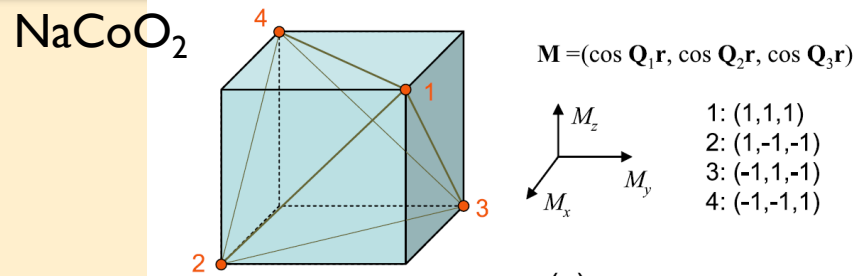
Theory: AHE in AFM



Shindou & Nagaosa PRL (2001).



Chen, Niu, MacDonald, PRL (2014).



What is the order parameter behind AHE?

Magnetic Multipoles vs. Cluster Multipoles

Suzuki, Arita et al., PRB 094406(2017).

Magnetic multipoles

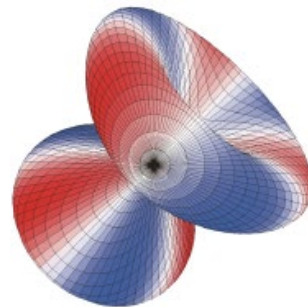
$$M_{\ell m} = \sqrt{\frac{4\pi}{2\ell + 1}} \int d\mathbf{r} \nabla_i (r^\ell Y_{\ell m}(\hat{\mathbf{r}})^*) \cdot \mathbf{m}(\mathbf{r})$$

↓
Magnetization density around an atom

Magnetic dipole



Magnetic octupole



Characterize the magnetization density around an atom

Symmetry
properties

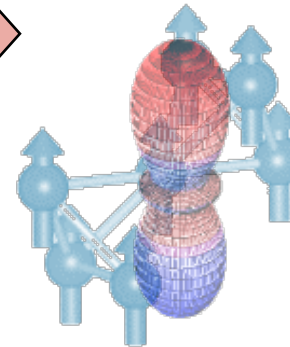
Cluster multipoles (CMP)

$$M_{\ell m} \equiv \sqrt{\frac{4\pi}{2\ell + 1}} \sum_{i=1}^N \nabla_i (R_i^\ell Y_{\ell m}(\hat{R}_i)^*) \cdot \mathbf{m}_i$$

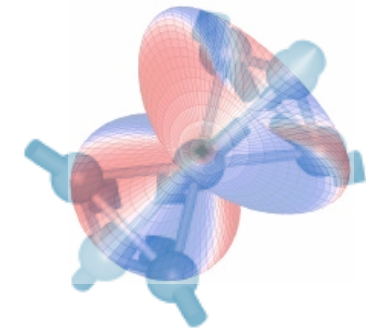
↓
magnetic moment of the i -th atom

Suzuki, RA, et al., PRB 95 094406(2017)

Cluster dipole (Ferromagnet)



Cluster octupole (Antiferromagnet)

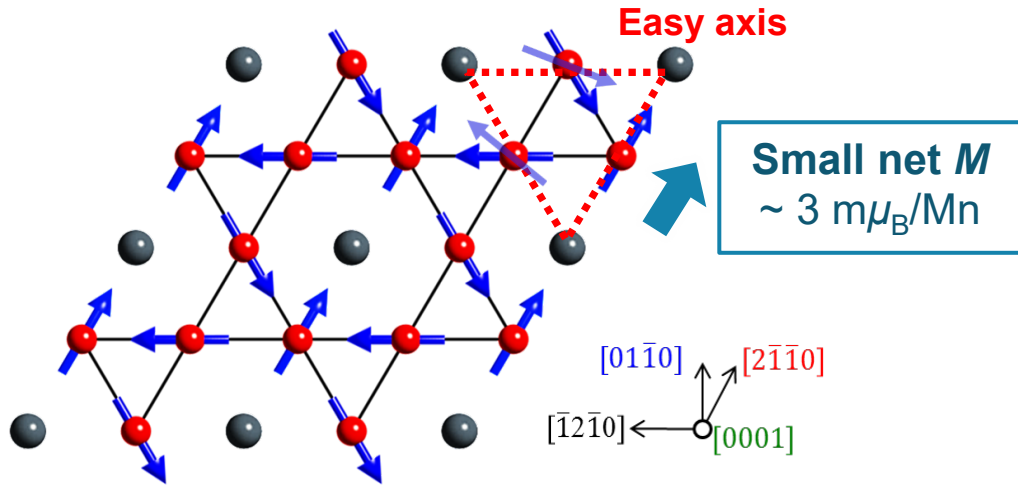


Characterize the magnetic configuration for a cluster of atoms

CMP: A new basis for classifying antiferromagnetic structures

Large room-temperature AHE in AFM Mn₃Sn

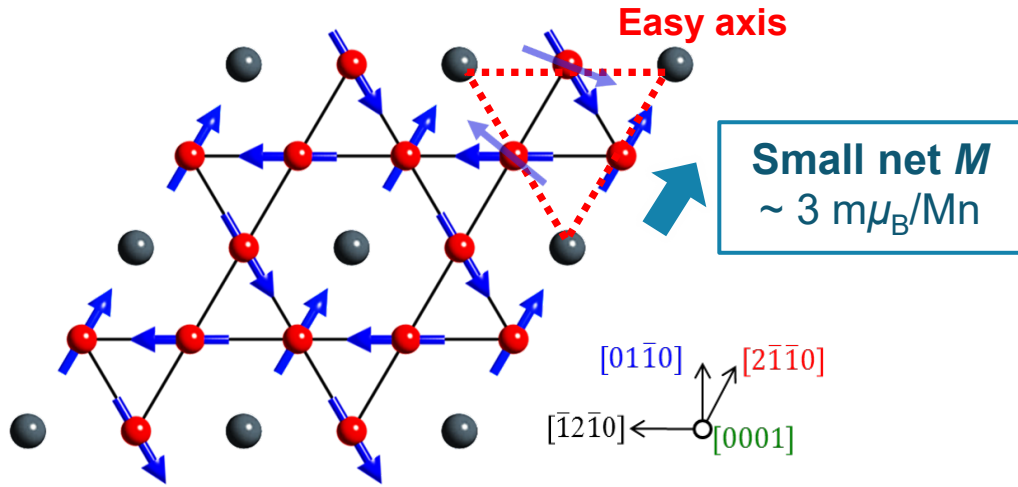
Noncollinear AFM order at $T_N = 430$ K



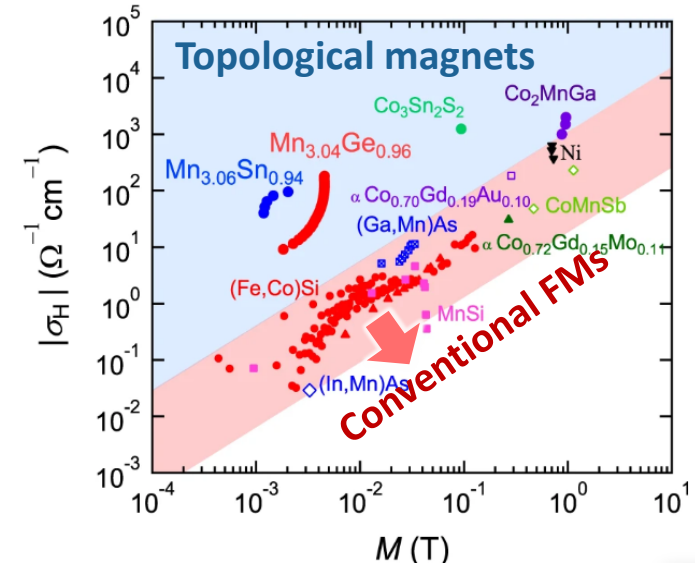
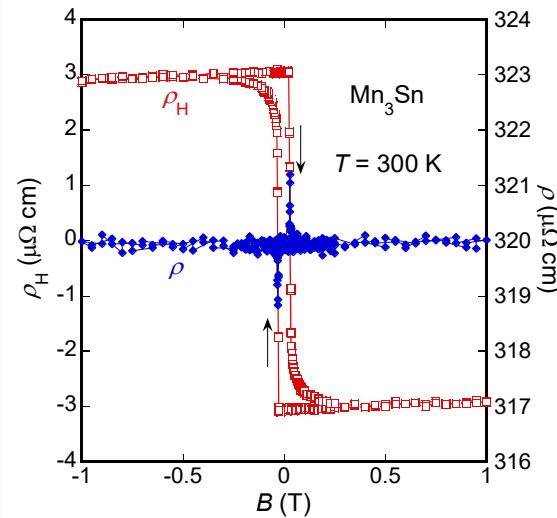
$$\rho_H = R_0 B + R_S \mu_0 M \sim 0.01 \mu\Omega\text{cm}$$

Large room-temperature AHE in AFM Mn₃Sn

Noncollinear AFM order at $T_N = 430$ K



Large AHE well beyond the linear-in- M relation for conventional FMs

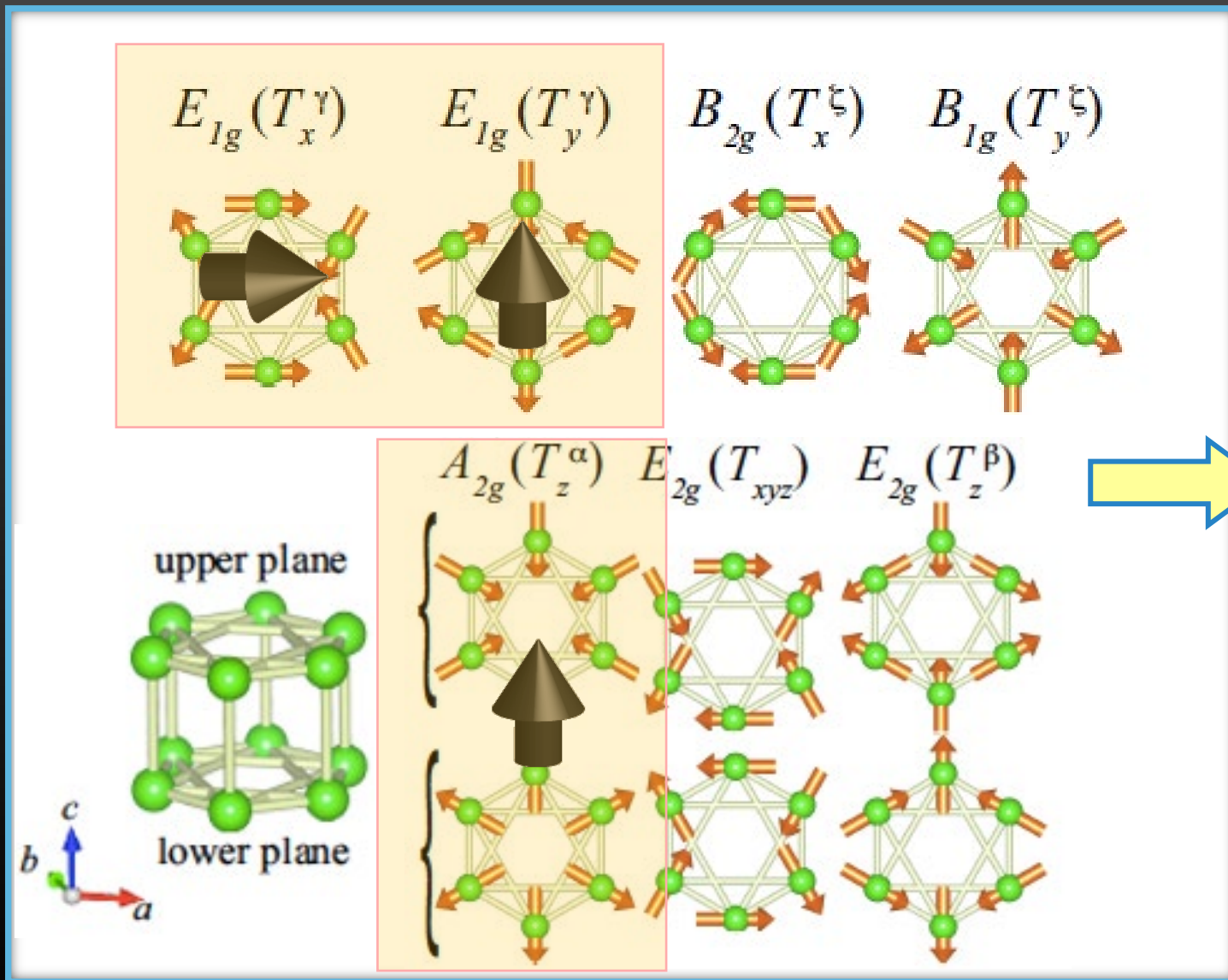


S. N., N. Kiyohara, T. Higo, *Nature* (2015)

$$\rho_H = R_0 B + R_S \mu_0 M \sim 0.01 \mu\Omega \text{ cm} \quad \text{vs.} \quad \rho_H = R_0 B + R_S \mu_0 M + \rho_H^{\text{AF}} \sim 3 \mu\Omega \text{ cm}$$

The large AHE arises from a momentum-space fictitious field (i.e., Berry curvature) instead of the net M

Cluster octupoles in AFM Mn₃Sn

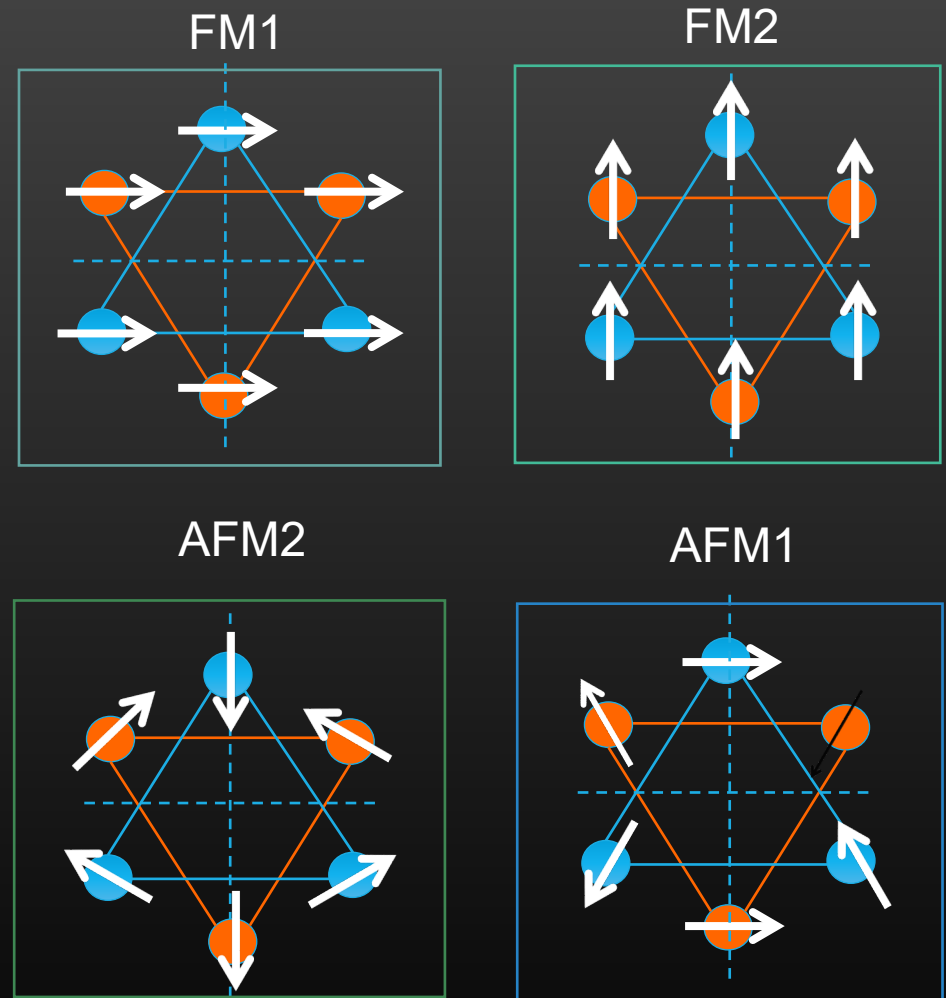


These cluster octupoles behave like a magnetic dipole under time reversal, mirror reflection, and spatial inversion operations

Octupolar polarization plays the same role as M in FMs.

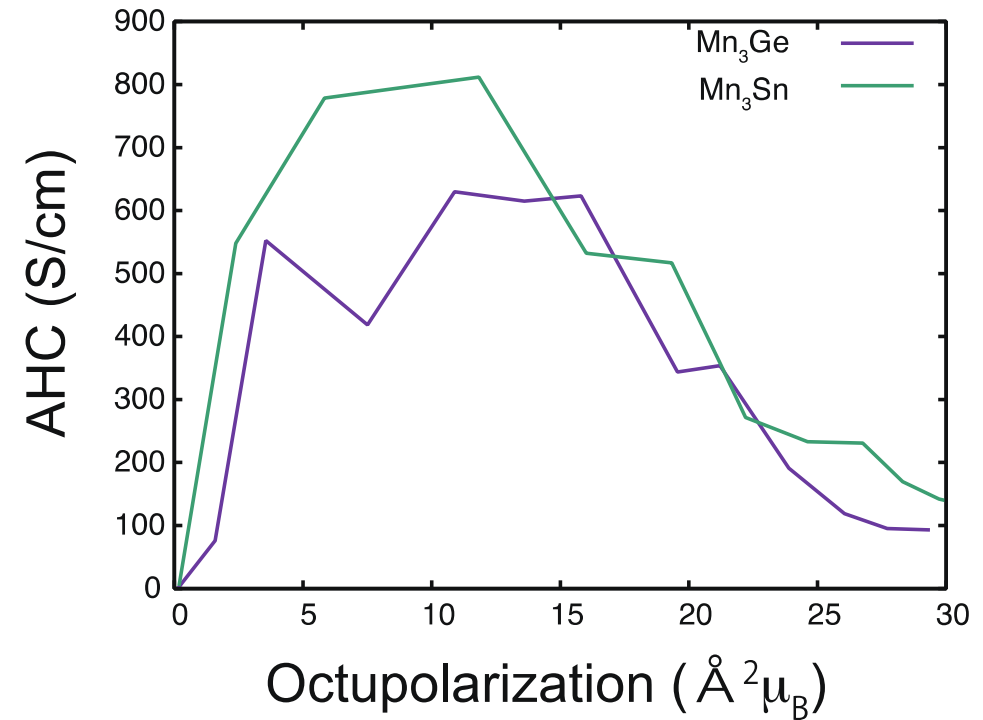
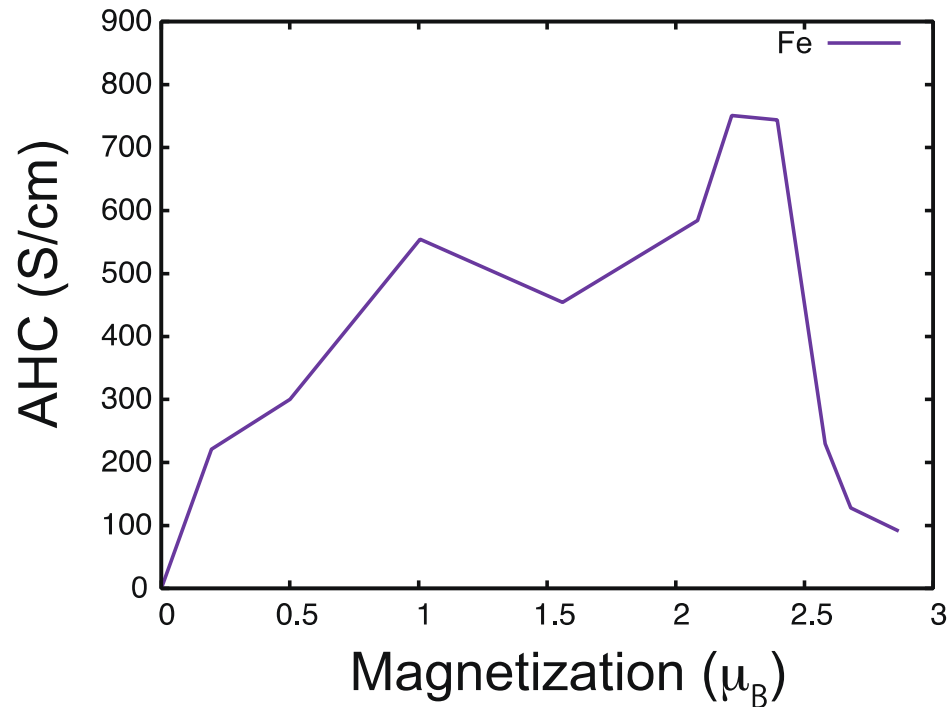
Cluster octupoles in AFM Mn₃Sn

IREP	CMP
A_{2g}	$J_z \equiv M_{10}$
E_{1g}	$J_x \equiv \frac{1}{\sqrt{2}}(-M_{11} + M_{1-1})$ $J_y \equiv \frac{i}{\sqrt{2}}(M_{11} + M_{1-1})$
A_{1u}	$Q_{3z^2-r^2} \equiv M_{20}$
E_{2u}	$Q_{x^2-y^2} \equiv \frac{1}{\sqrt{2}}(M_{22} + M_{2-2})$ $Q_{xy} \equiv \frac{i}{\sqrt{2}}(-M_{22} + M_{2-2})$
E_{1u}	$Q_{zx} \equiv \frac{1}{\sqrt{2}}(-M_{21} + M_{2-1})$ $Q_{yz} \equiv \frac{i}{\sqrt{2}}(M_{21} + M_{2-1})$
A_{2g}	$T_z^\alpha \equiv M_{30}$
E_{1g}	$T_x^\gamma \equiv \frac{1}{\sqrt{2}}(-M_{31} + M_{3-1})$ $T_y^\gamma \equiv \frac{i}{\sqrt{2}}(M_{31} + M_{3-1})$
E_{2g}	$T_{xyz} \equiv \frac{i}{\sqrt{2}}(-M_{32} + M_{3-2})$ $T_z^\beta \equiv \frac{1}{\sqrt{2}}(M_{32} + M_{3-2})$
B_{2g}	$T_x^\zeta \equiv \frac{1}{\sqrt{2}}(-M_{33} + M_{3-3})$
B_{1g}	$T_y^\zeta \equiv -\frac{i}{\sqrt{2}}(M_{33} + M_{3-3})$



AF structure in Mn₃Sn = ferroic order of octupoles with the E_{1g} representation

Anomalous Hall effect in Mn_3Sn within the framework of CMP

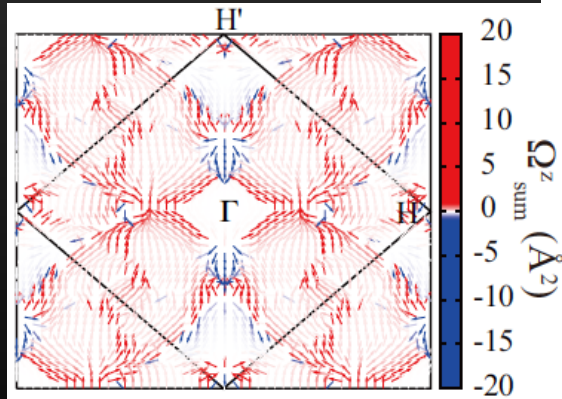
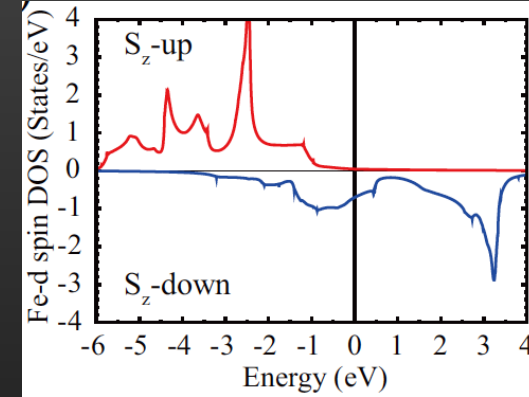
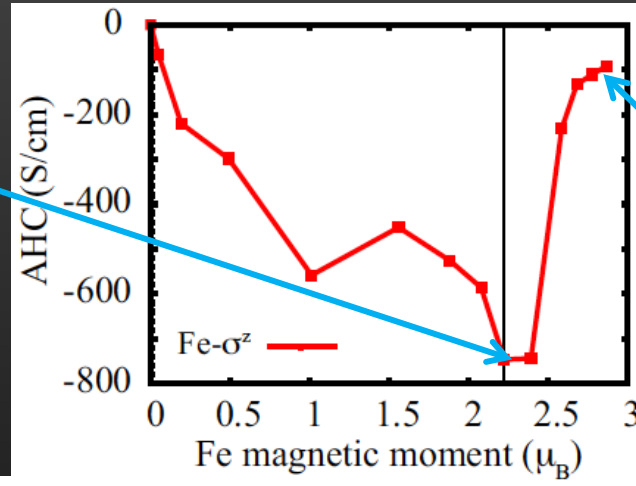
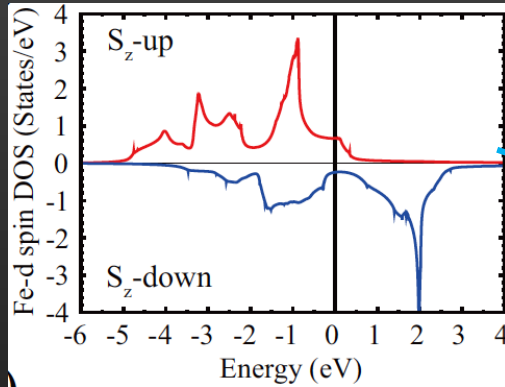


The cluster multipole theory allows us to discuss anomalous Hall conductivity (AHC) in FM and AFM with a unified framework

Cluster multipoles can effectively characterize the magnetic and transport properties of AFM

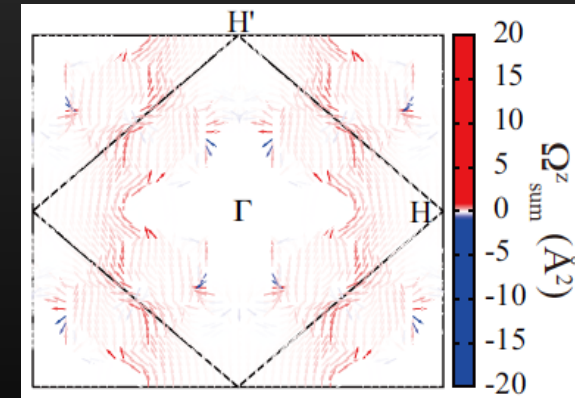
AHE and spin splitting of bcc-Fe

FM states of bcc-Fe



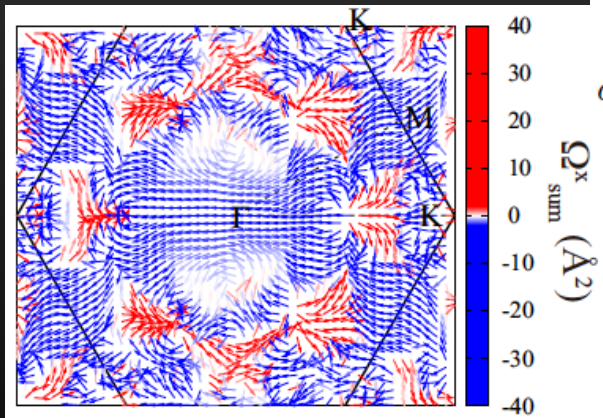
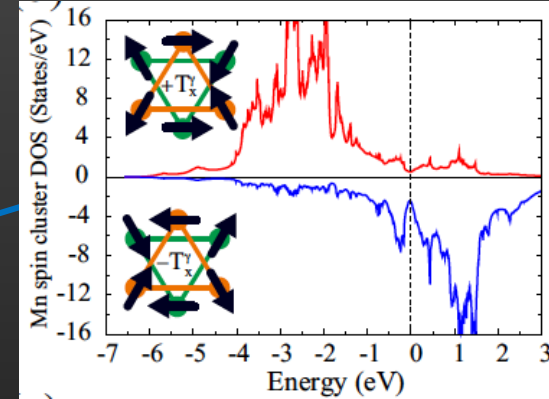
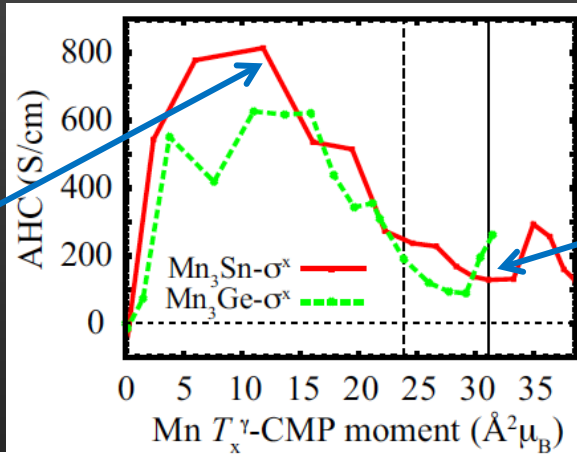
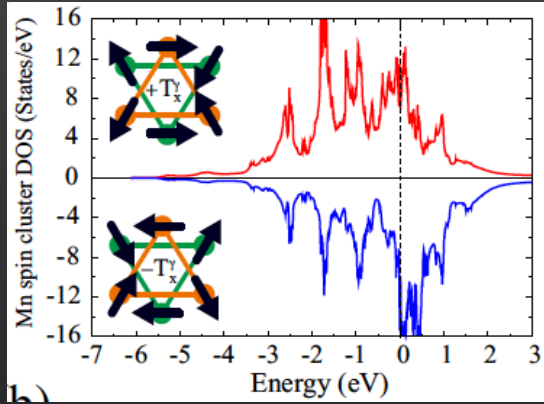
$$\sigma^z = -\frac{e^2}{\hbar} \int \frac{dk}{(2\pi)^3} \sum_n f(\varepsilon_n(\mathbf{k}) - \mu) \Omega_n^z(\mathbf{k})$$

$$\Omega_{\text{sum}}^z(\mathbf{k})$$



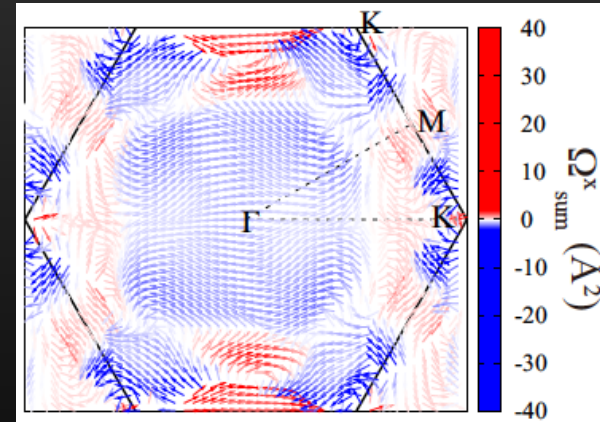
AHE and CMP orbital splitting of Mn₃Sn

AFM states of Mn₃Z (Z=Sn, Ge)



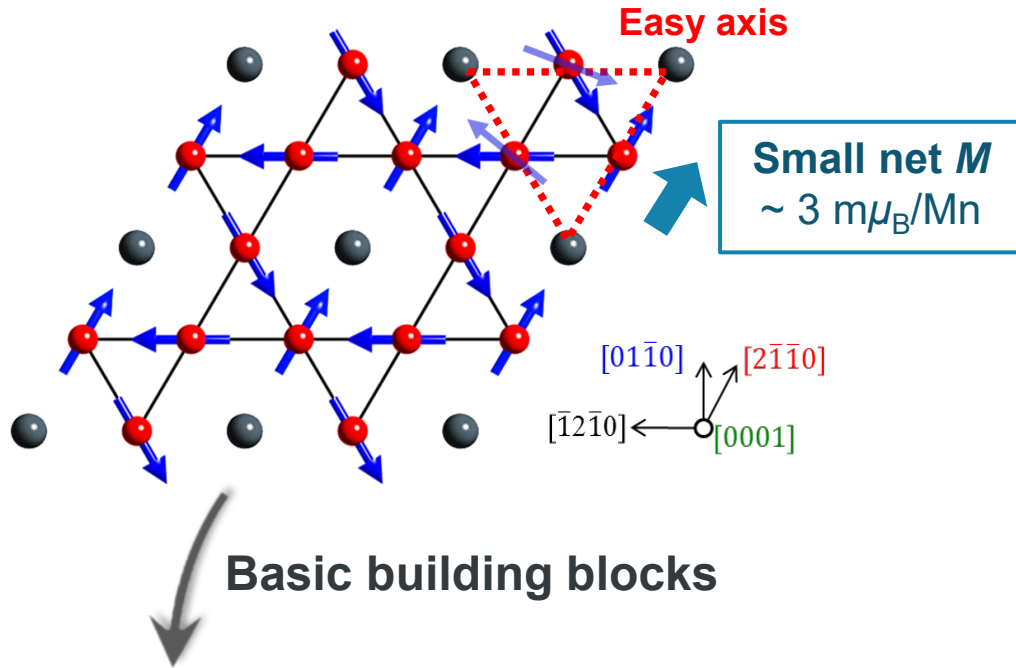
$$\sigma^x = -\frac{e^2}{\hbar} \int \frac{dk}{(2\pi)^3} \sum_n f(\varepsilon_n(\mathbf{k}) - \mu) \Omega_n^x(\mathbf{k})$$

$$\Omega_{\text{sum}}^x(\mathbf{k})$$



Summary: Cluster octupole ordering in Mn₃Sn

Noncollinear AFM order at $T_N = 430$ K

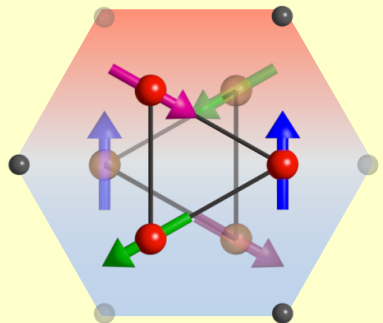


A group of six spins forms a cluster octupole moment, which is highly tunable by a magnetic field, electrical current, and strain.

The AFM order in Mn₃Sn is a ferroic order of cluster octupoles, which macroscopically breaks time-reversal symmetry.

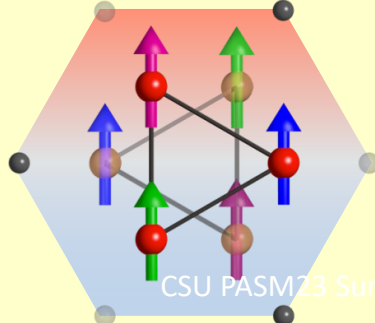
Cluster octupole polarization $K \sim$ Berry Curvature (the momentum-space fictitious magnetic field)

Magnetic Octupole



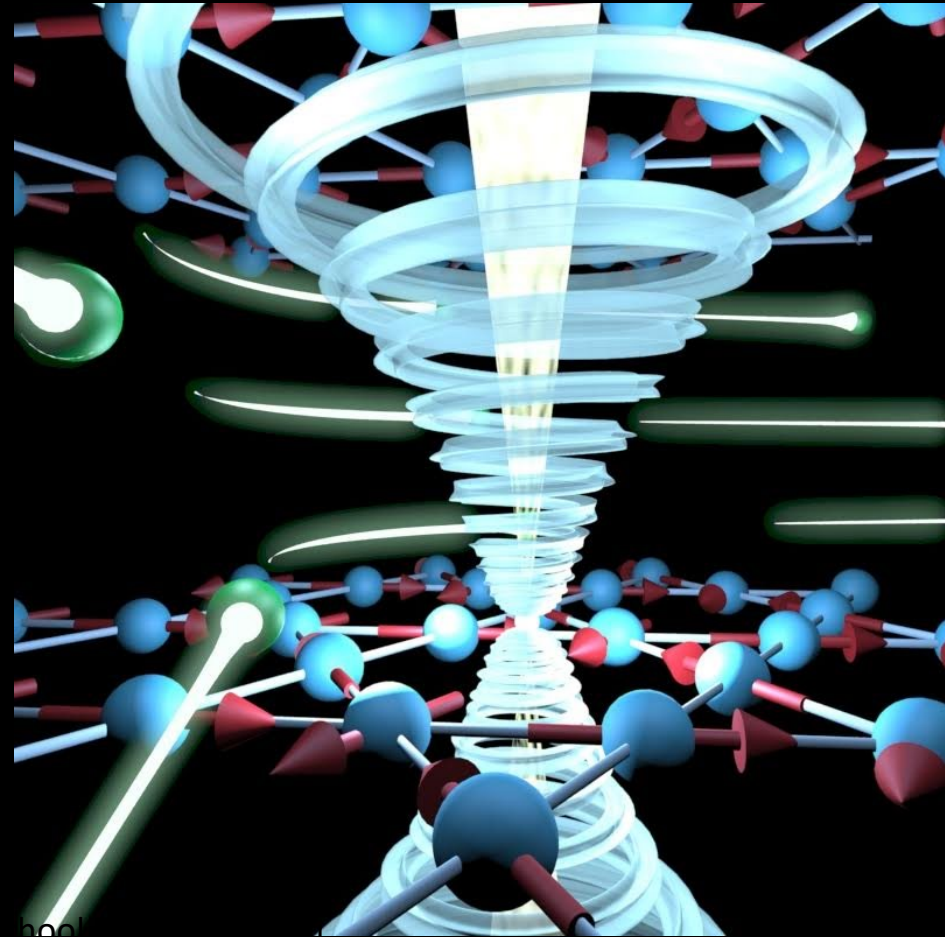
=

Magnetic Dipole



$$\sigma_{\alpha\beta}^H = \frac{e^2}{2\pi h} \epsilon_{\alpha\beta\gamma} K_\gamma$$

Strain Control of AHE in Mn_3Sn



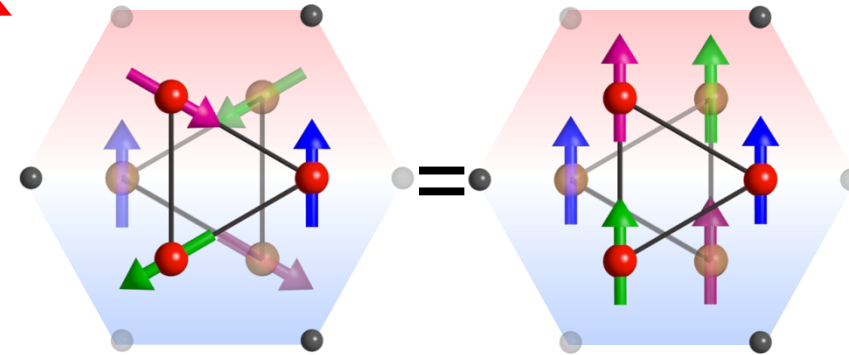
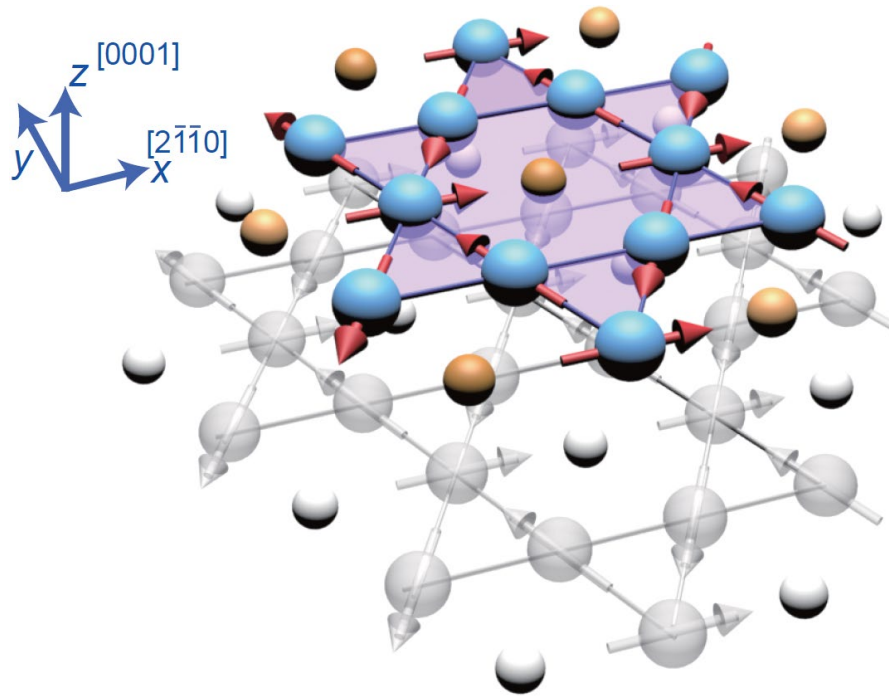
Nature Physics volume 18, 1086–1093 (2022)

Magnetic Multipole



Suzuki, Arita et al., PRB 094406(2017).

NonCollinear AFM $T_N = 430$ K



AF

Dipole
(Rank = 1)

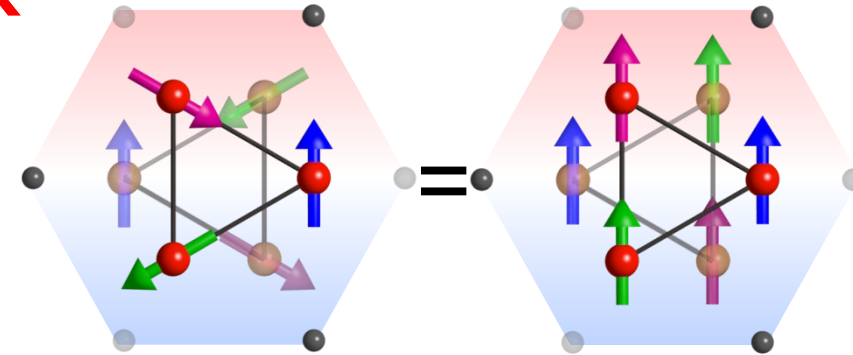
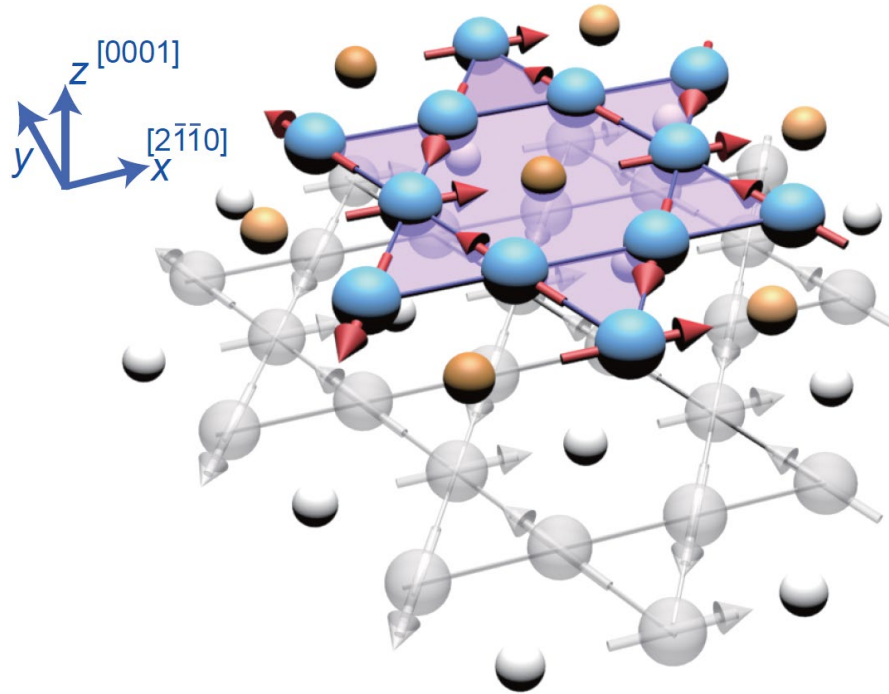
The Same Mag. Space Group
Breaking Time Reversal Symm.

Magnetic Octupole



Suzuki, Arita et al., PRB 094406(2017).

NonCollinear AFM $T_N = 430$ K



Magnetic Octupole
(Rank = 3)

Dipole
(Rank = 1)

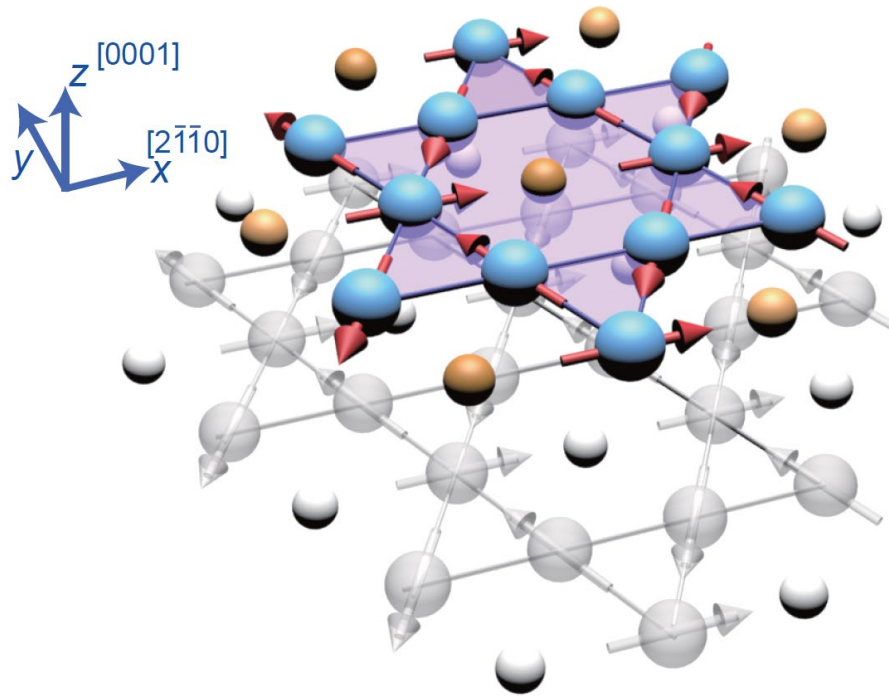
The Same Mag. Space Group
Breaking Time Reversal Symm.

Magnetic Octupole



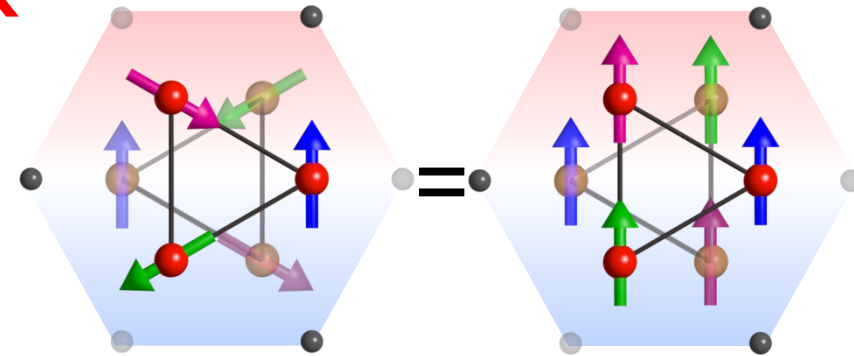
Suzuki, Arita et al., PRB 094406(2017).

NonCollinear AFM $T_N = 430$ K



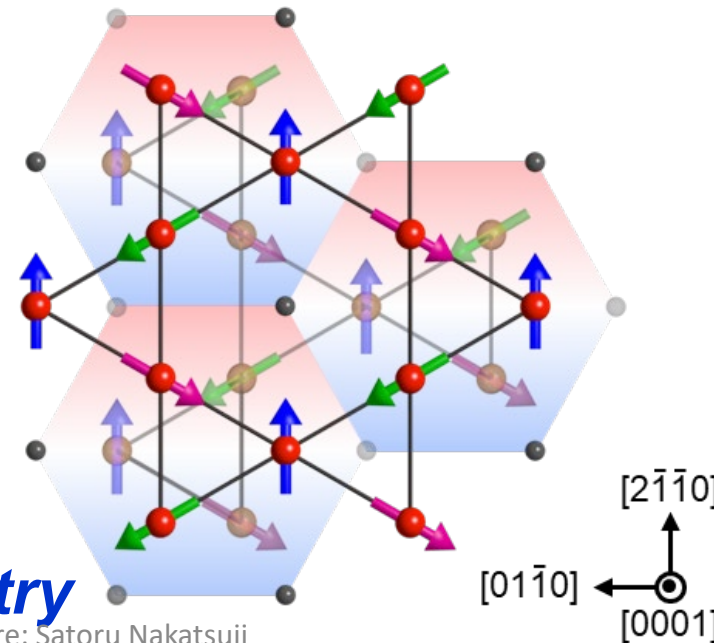
*Ferroic Order of
Magnetic Octupole*

Breaking Time Reversal Symmetry



Magnetic Octupole

FM

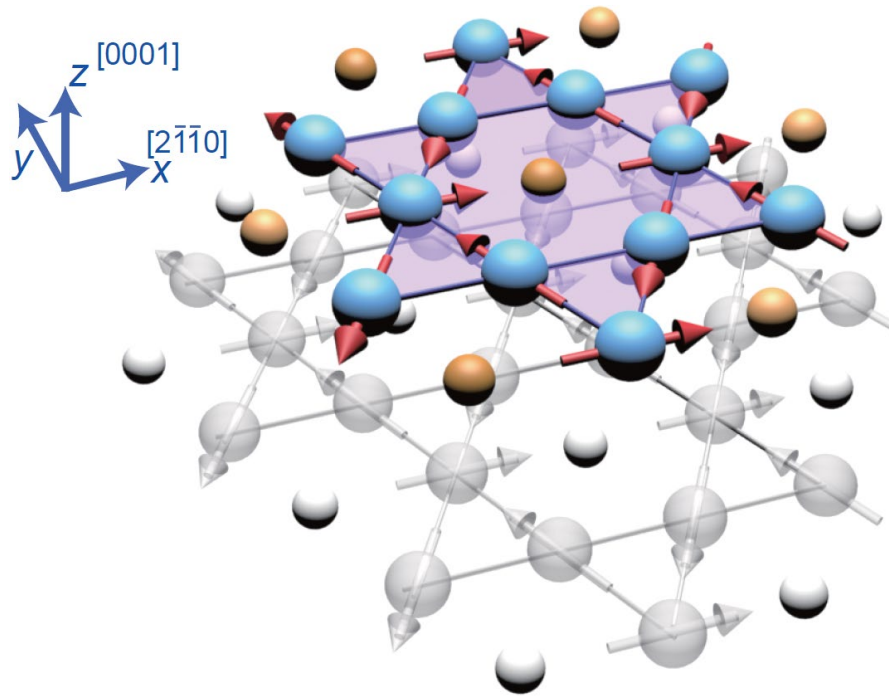


Magnetic Octupole

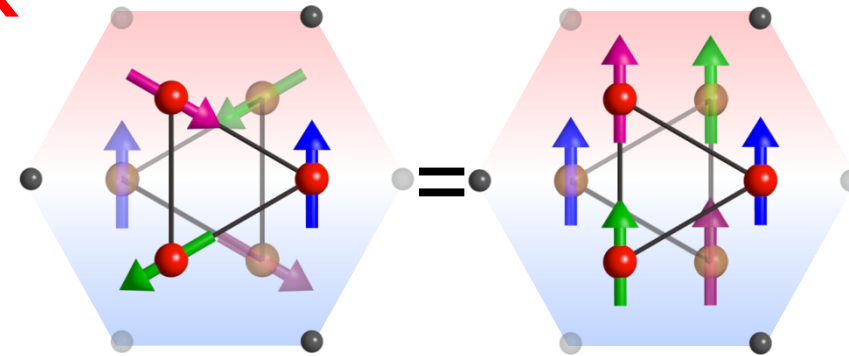


Suzuki, Arita et al., PRB 094406(2017).

NonCollinear AFM $T_N = 430$ K



*Ferroic Order of
Magnetic Octupole*



Magnetic Octupole

FM

**K : octupole polarization
~ Berry Curvature**

$$\sigma_{\alpha\beta}^H = \frac{e^2}{2\pi h} \epsilon_{\alpha\beta\gamma} K_\gamma$$

Breaking Time Reversal Symmetry

Piezomagnetic effect in antiferromagnets

□ For certain types of antiferromagnets, strain breaks the symmetry between magnetic sublattices, and induces net magnetization linear in the applied strain

□ Piezomagnetic effect :

$$\begin{pmatrix} M_x \\ M_y \\ M_z \end{pmatrix} = \begin{pmatrix} \Lambda_{11} & \Lambda_{12} & \Lambda_{13} & \Lambda_{14} & \Lambda_{15} & \Lambda_{16} \\ \Lambda_{21} & \Lambda_{22} & \Lambda_{23} & \Lambda_{24} & \Lambda_{25} & \Lambda_{26} \\ \Lambda_{31} & \Lambda_{32} & \Lambda_{33} & \Lambda_{34} & \Lambda_{35} & \Lambda_{36} \end{pmatrix} \begin{pmatrix} \sigma_{xx} \\ \sigma_{yy} \\ \sigma_{zz} \\ \sigma_{yz} \\ \sigma_{xz} \\ \sigma_{xy} \end{pmatrix}$$

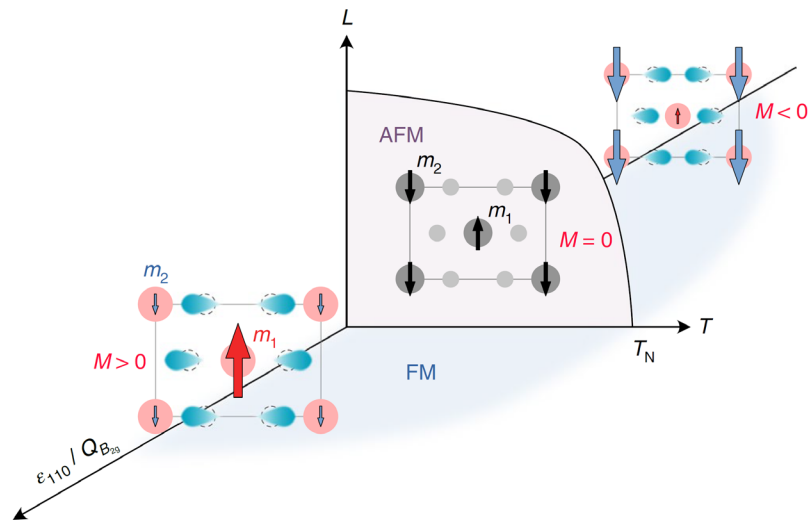
□ Λ is non-zero for AFM that macroscopically break time reversal symmetry or preserve time reversal symmetry *only* in combination with rotation and reflection. 66 out of 122 magnetic point groups allow piezomagnetic effect

E. Dzyaloshinskii, JETP 33, 807 (1957) B. A. Tavger and V. M. Zaitzev, *J. Exp. Theor. Phys.* 3 (1956)

Piezomagnetic effect in collinear antiferromagnet CoF_2 and MnF_2

- Tetragonal structure, 2 distinct transition metal sites
- Strain along [110] direction, breaks the symmetry of the sublattice moments \rightarrow ferrimagnetic moment along [001]

Moriya, T., *Journal of Physics and Chemistry of Solids* **11** (1959)



S. A. Disa, *et al. Nature Physics* **16** (2020)

- In the presence of piezomagnetic effect, under a constant field, a static stress can mediate 180° AF domain reversal

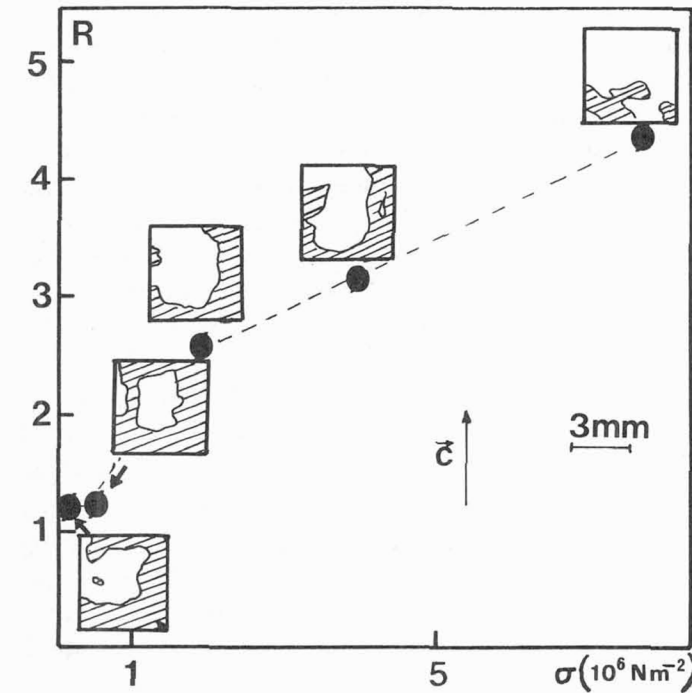


Fig. 1. — Flipping ratio R as a function of the stress applied during the cooling of the MnF_2 crystal ($4 \times 4 \times 2.5 \text{ mm}^3$) through T_N in a 0.01 T magnetic field, and schematic drawing of the topographs recorded after removing the field, at 20 K, with neutrons polarized along [001].

Baruchel, J., *et al. Le Journal de Physique Colloques* **49** (1988)

Has been seen mostly in AF insulators

Piezomagnetic effect in Weyl semimetal Mn_3Sn

□ The magnetic structure of 120° antichiral phase macroscopically breaks time-reversal symmetry, piezomagnetic effects are allowed

□ Its magnetic point group symmetry ($m'm'm'$) dictates:

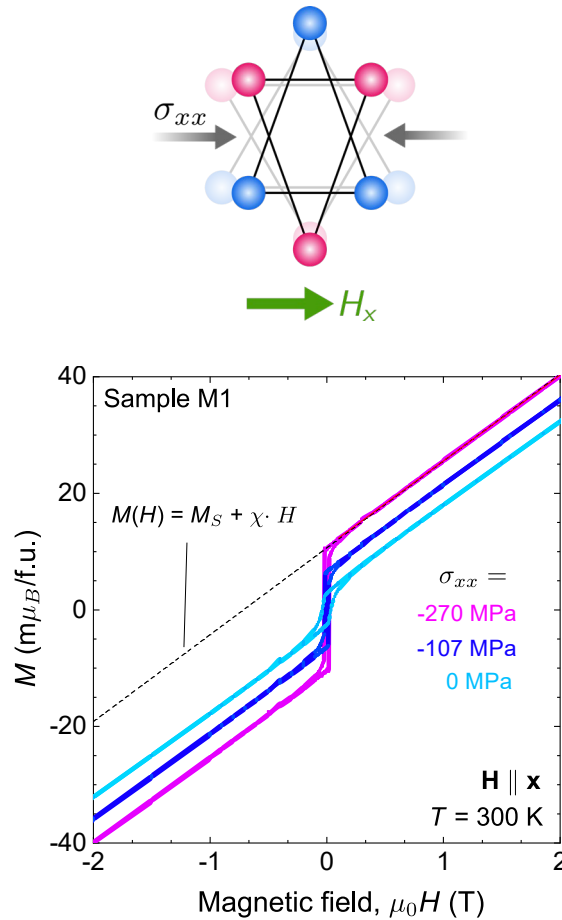
$$\begin{pmatrix} M_x \\ M_y \\ M_z \end{pmatrix} = \begin{pmatrix} \Lambda_{11} & \Lambda_{12} & \Lambda_{13} & 0 & 0 & \Lambda_{16} \\ \Lambda_{21} & \Lambda_{22} & \Lambda_{23} & 0 & 0 & \Lambda_{26} \\ 0 & 0 & 0 & \Lambda_{34} & \Lambda_{35} & 0 \end{pmatrix} \begin{pmatrix} \sigma_{xx} \\ \sigma_{yy} \\ \sigma_{zz} \\ \sigma_{yz} \\ \sigma_{xz} \\ \sigma_{xy} \end{pmatrix}$$

Source: Bilbao crystallographic server

□ In-plane stress couples to magnetization,

$$\text{for example } M_x = \Lambda_{11}\sigma_{xx} + \Lambda_{12}\sigma_{yy} + \Lambda_{16}\sigma_{xy}$$

Magnetization of Mn₃Sn under in-plane uniaxial compression



□ We fit the data with:

$$M(H) = M_S + \chi H$$

Spontaneous
component

Field-induced
component

→ M_S is enhanced by in-plane stress

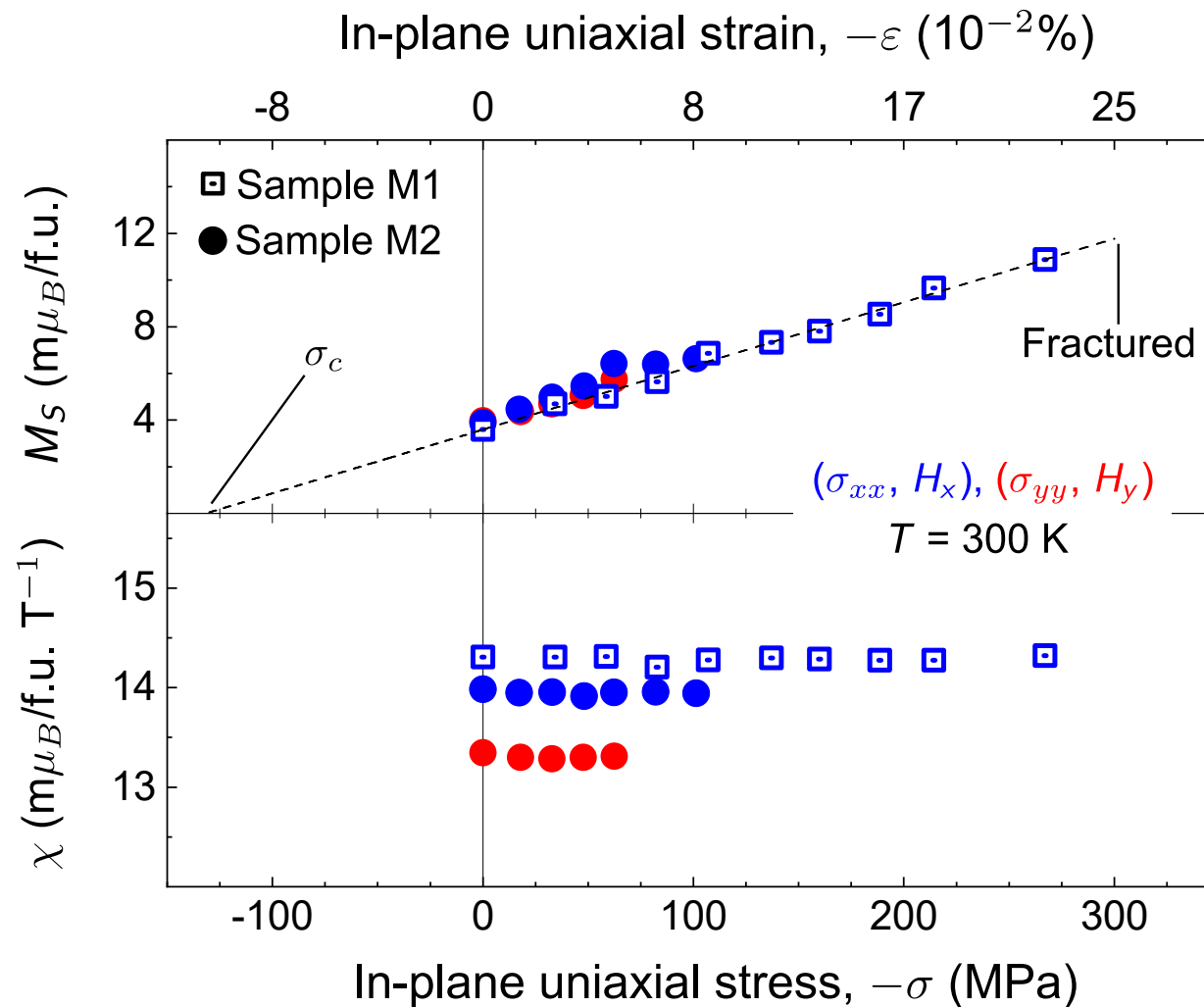
→ χ is insensitive to stress

Stress-dependence of spontaneous magnetization M_S

$$M_S = M_S(\sigma = 0) + \Lambda_{11}\sigma_{xx}$$

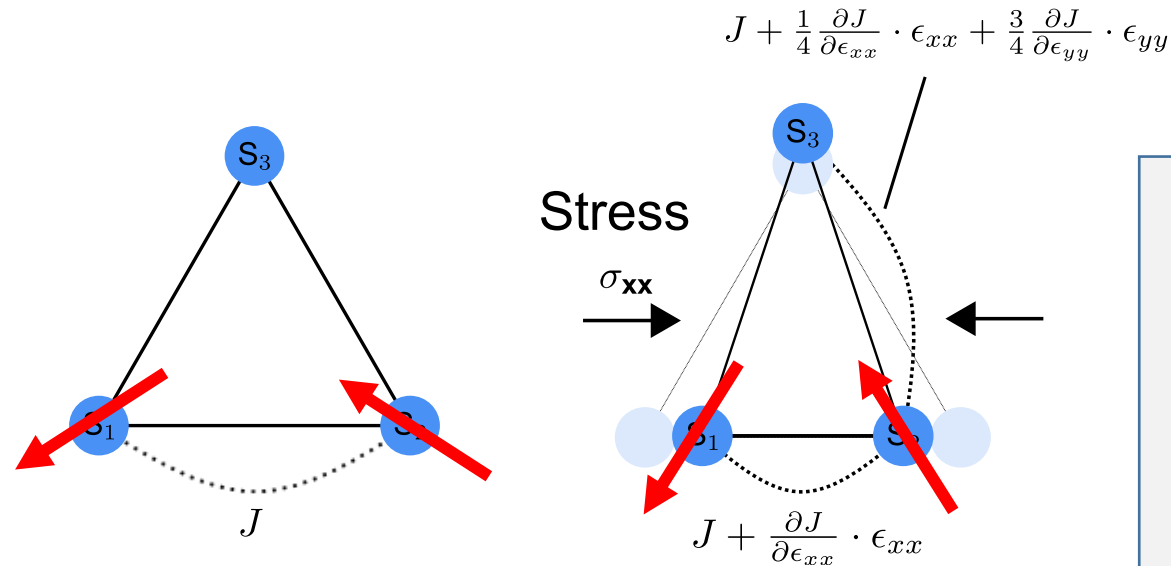
→ Evidence for piezomagnetism

$$\square |\Lambda_{11}| \sim 0.027 \text{ m}\mu_B/\text{f.u. GPa}^{-1} \text{ (0.078 Gauss/MPa)}$$



Microscopic origin of piezomagnetic effect in Mn₃Sn

□ Exchange interaction J depends on the distance between magnetic ions (*exchange striction*)



$$H'_{\text{ex}} = \sum_{i \neq j} J_{ij} (\mathbf{s}_i \cdot \mathbf{s}_j)$$

$$= H_{\text{ex}} + \Delta H_{\text{ex}}$$

ΔH_{ex} = Correction due to exchange striction

$$H_{\text{ex}} = J (\mathbf{s}_1 \cdot \mathbf{s}_2 + \mathbf{s}_2 \cdot \mathbf{s}_3 + \mathbf{s}_3 \cdot \mathbf{s}_1)$$

Illustration of piezomagnetic effect in Mn_3Sn

□ strain-dependent magnetization

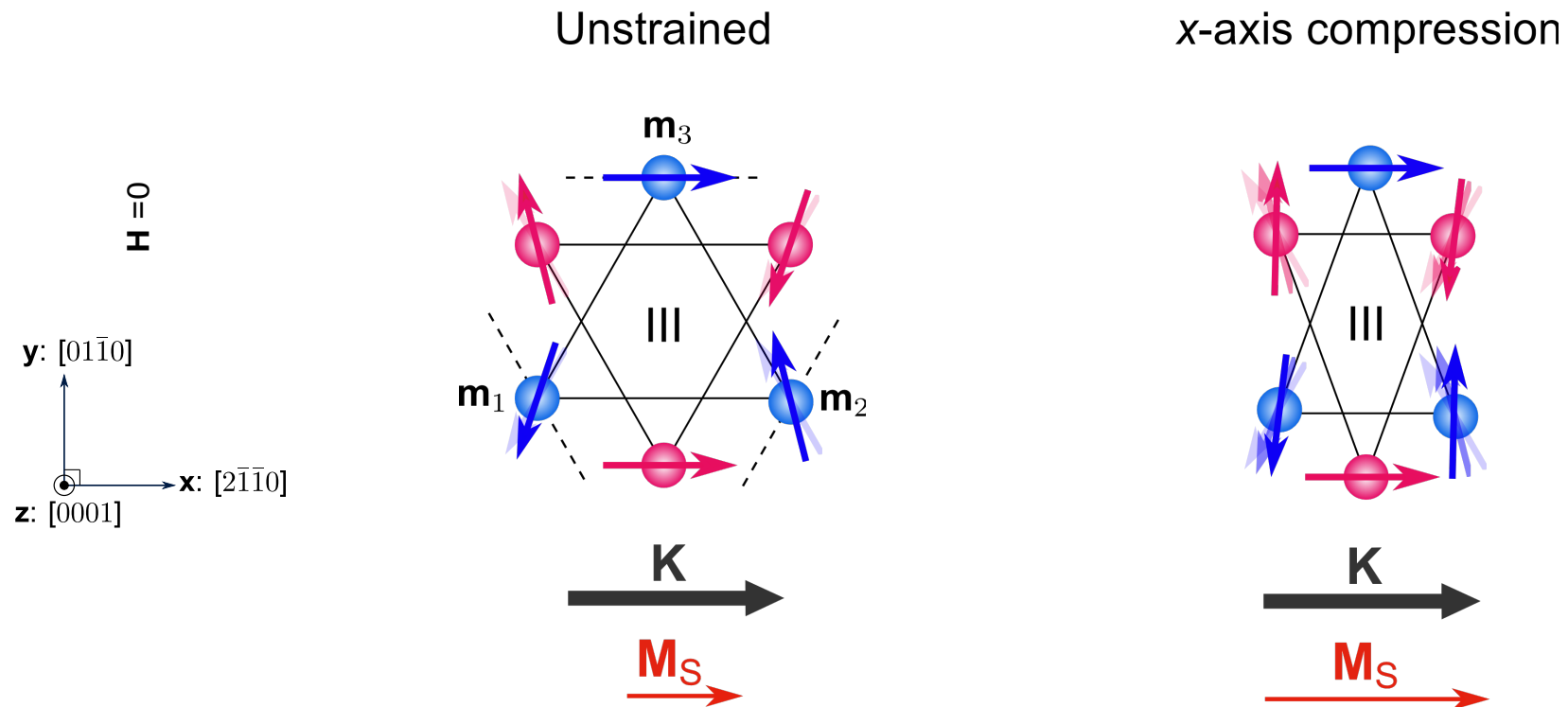
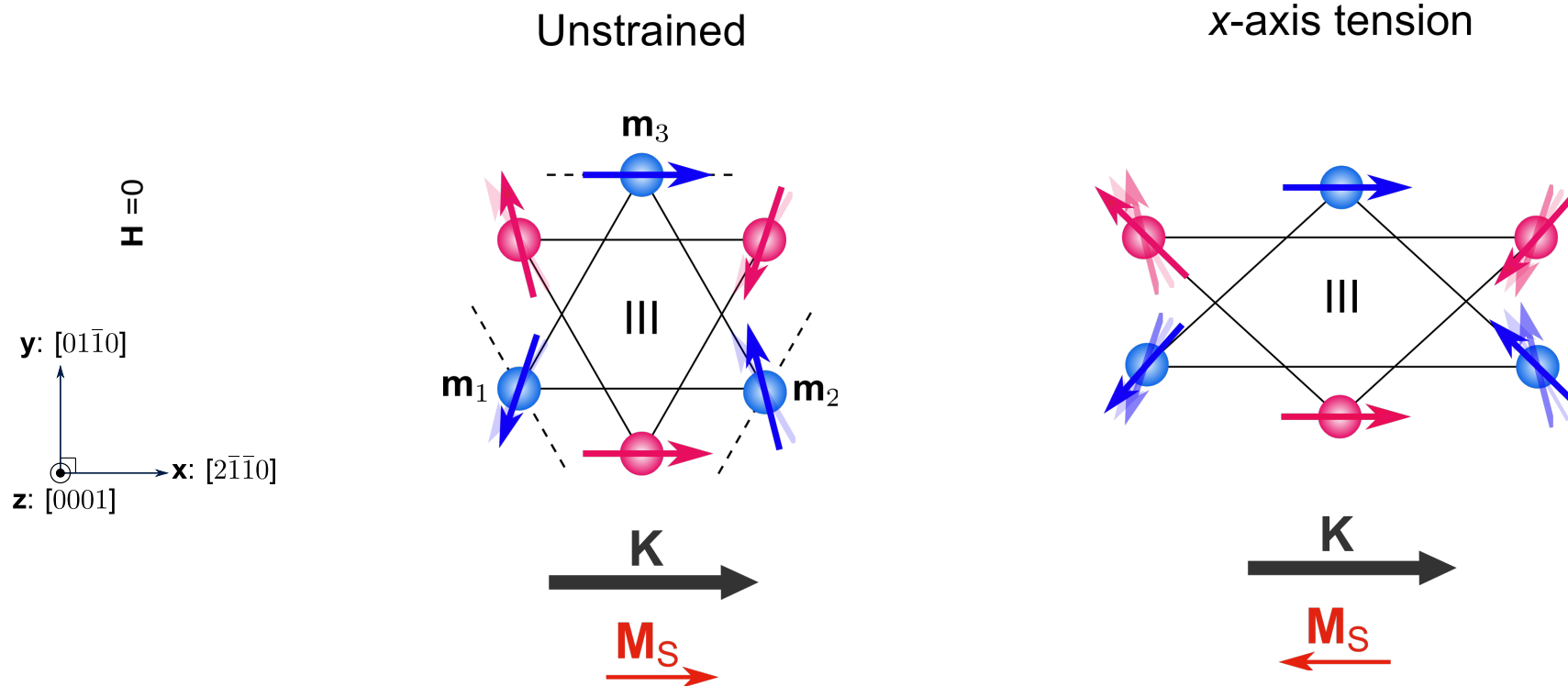


Illustration of piezomagnetic effect in Mn_3Sn

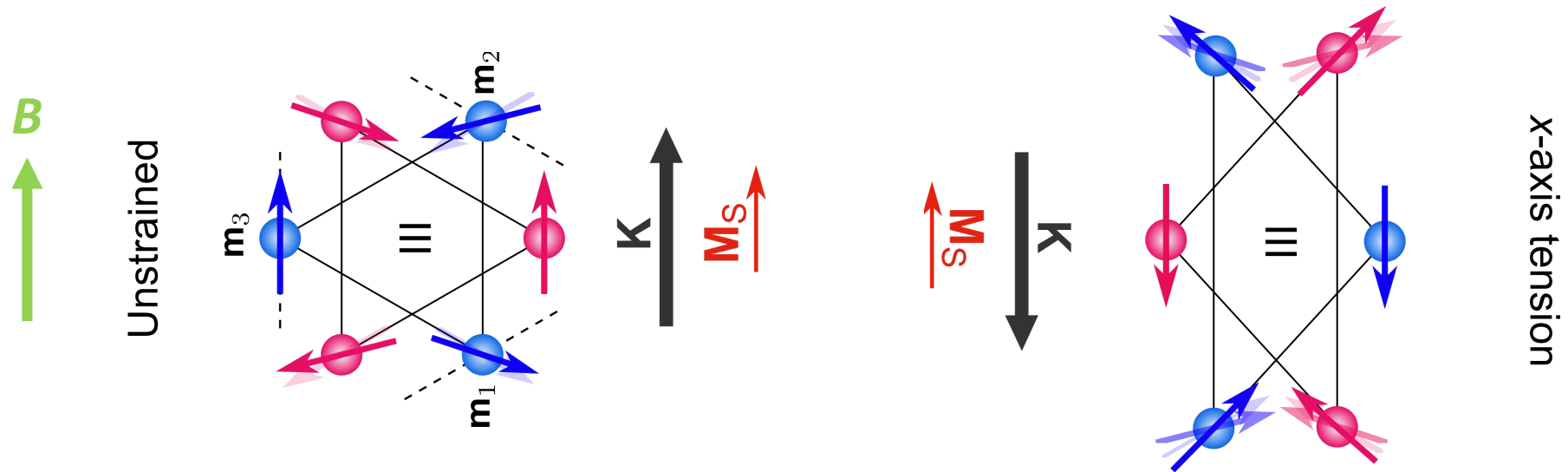
□ strain-dependent magnetization



□ In-plane tension may rotate \mathbf{M} to the opposite direction to \mathbf{K}

Illustration of piezomagnetic effect in Mn_3Sn

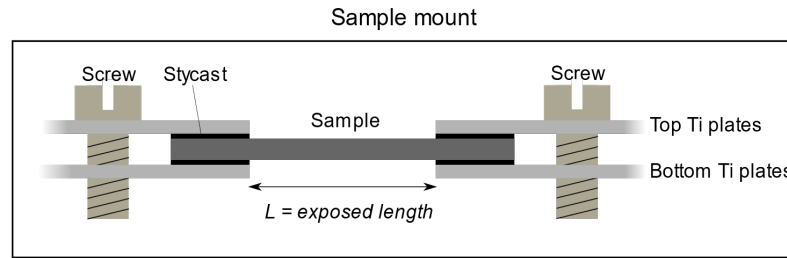
□ strain-dependent magnetization



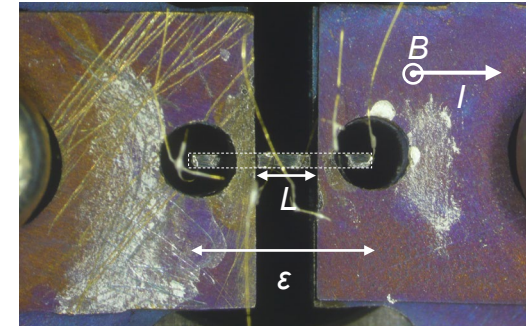
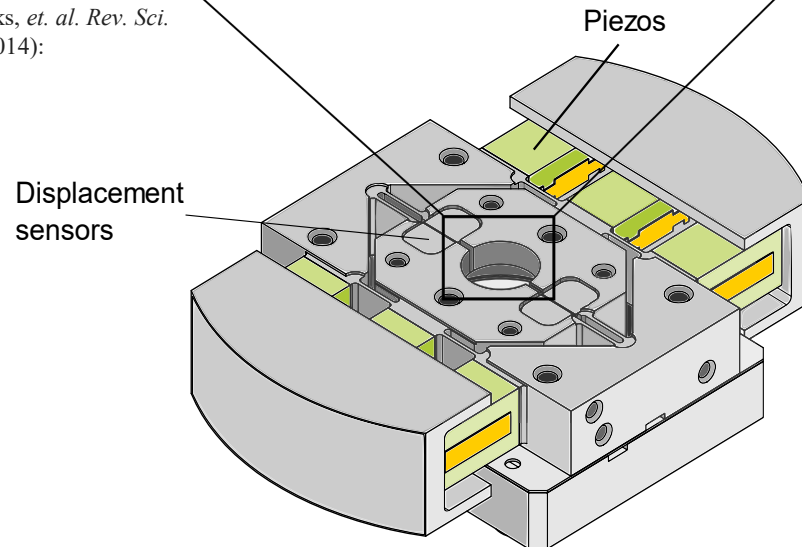
□ In-plane tension may rotate \mathbf{M} to the opposite direction to \mathbf{K}

→ Leads to a sign change in the anomalous Hall effect

Uniaxial strain cell and sample mounting



C.W. Hicks, *et. al. Rev. Sci. Ins.* **85** (2014):



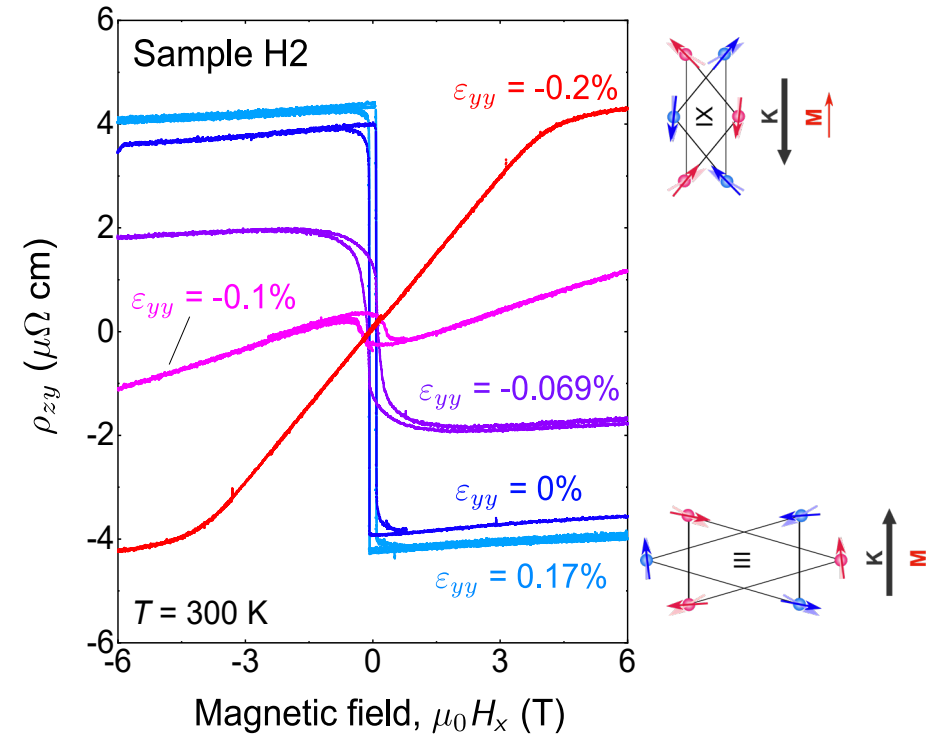
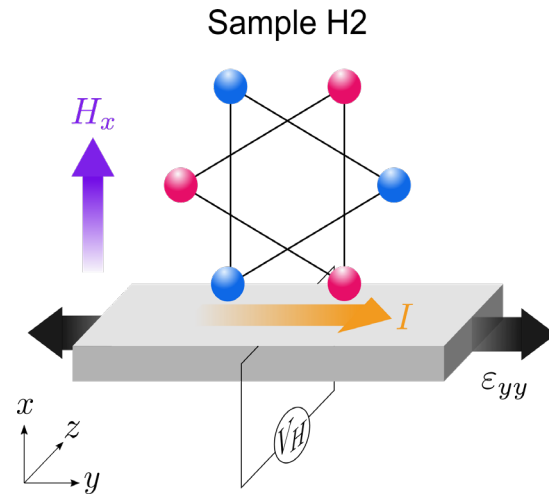
$$\text{Strain: } \varepsilon = \Delta L / L \quad \Delta L = \varepsilon_0 A \left(\frac{1}{C} - \frac{1}{C_0} \right)$$

A = area of parallel plate capacitor

C = capacitance of displacement sensor (pF)

C_0 = initial capacitance of displacement sensor (pF)

Anomalous Hall effect under in-plane uniaxial strain

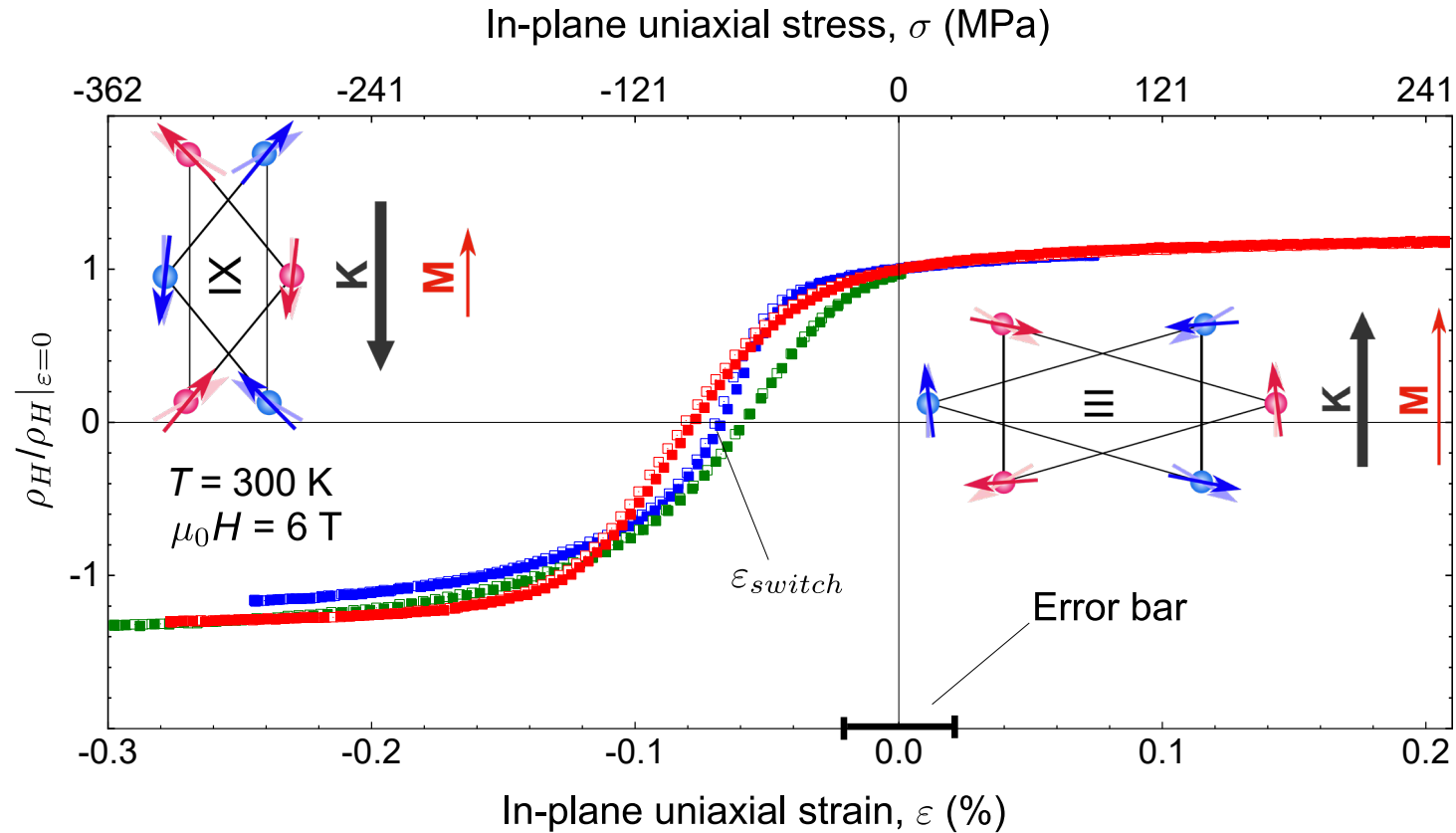
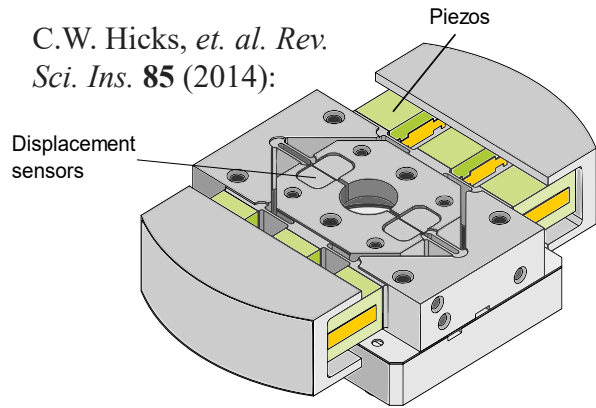


- AHE couples to in-plane uniaxial strain \rightarrow sign change of AHE under compressive strain

Strain dependence of normalized anomalous Hall resistivity



C.W. Hicks, *et. al. Rev. Sci. Ins.* **85** (2014):



□ Hall resistivity can change sign while the sign of the magnetization remains the same

→ Evidence that the AHE in Mn_3Sn is controlled by the octupolar order, and **not** the dipolar magnetization